Institute of Energy Plant Technology,

Ruhr-University Bochum,

Documentation of the models for simulating the combustion behaviour of refuse-derived-fuel (RDF) within the openFOAM / DEM framework

Contents

1 Models for describing the thermochemical conversion behaviour of RDF

The following sections describe models developed as part of the transfer project T1 of the transregio CRR/TRR 129 “Oxyflame – Development of models and methods for describing the combustion of solid fuels in an oxygen-fuel atmosphere” to simulate the various thermochemical conversion processes of RDF. The models represent an improvement on the previous Ansys FLUENT® RDF models (rdf_udf_doku_website_englisch_final.pdf) in terms of predicting the conversion behaviour under superstoichiometric oxy-fuel conditions. In contrast to Ansys FLUENT®, where user-defined functions (UDFs) were used to couple the particle and fluid phases, the DEM code framework (discrete element methods) developed as part of TRR 287: BULK-REACTION is used for this purpose to enable the convenient usage of openFOAM for the simulations.

1.1 Overview of the various conversion processes

The basis for the various conversion processes is the thermal heating of the particle due to radiation and convection (see Figure 1(a)). Depending on the respective conversion step, endothermic and exothermic processes also influence the heat balance of the particle. As a result of the thermal thickness, this results in a temperature profile along the shells of the discretized particle. As soon as the temperature of a shell reaches or exceeds a specific temperature, the corresponding conversion process takes place (see Figure 1 (b)). Discretization is performed using finite differences, with one point representing one shell. A detailed description of the process can be found in the section on heating within this chapter. In contrast to Ansys FLUENT® RDF models, RDF is approximated here as a flat plate rather than a sphere of equal volume due to its flat shape. Figure 1 (b) shows a schematic representation of the conversion behavior for a biogenic particle; synthetic particles are converted according to the same principle, with a characteristic conversion temperature defined as the starting point for the process. Depending on the synthetic material, conversion steps may need to be added or removed. Due to the high proportion of polyethylene (PE) and polyvinyl chloride (PVC) in the total waste volume and the influence of PVC on material cycles in the cement manufacturing process, the modeling of the synthetic fraction focuses on these two materials. In view of the fact that no pronounced melting process is observed for PVC compared to PE due to the comparatively narrow temperature range between the melting and decomposition temperatures, separate modeling of the melting process for PVC has been omitted. In addition, the drying process is not modeled due to the negligible moisture content of plastics. Table 1 summarizes the conversion steps for residual char-forming and non-residual char-forming materials and provides information on the simulation approaches used. The term “thermal decomposition” has been

introduced due to the fact that, according to Liedmann [1], the release of volatiles in PE only occurs from the melting of the particle and is intended to distinguish it from pyrolysis, which in this modeling approach assumes the release of volatiles from the solid material. However, the underlying physical processes are identical. The conversion steps are not strictly sequential, but can take place simultaneously. Detailed information on the respective steps is explained in the following sections.

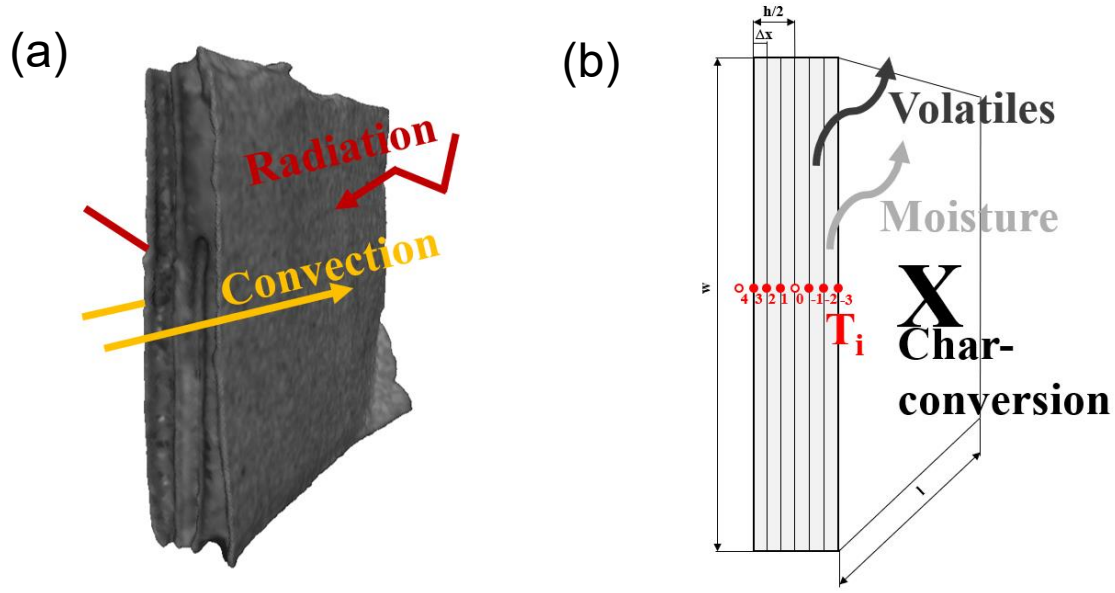

Figure 1: Modeling of the various thermochemical conversion processes for a biogenic particle: (a) heating; (b) conversion [2].

Table 1: Implemented models for simulating the thermochemical conversion of RDF.

Conversion step	Char-forming fractions **(paper & cardboard, textiles, PVC)**	Non-char-forming fractions **(PE)**	Simulation approach
1.	Heating	Heating	1D-heat conduction with Crank-Nicolson-method
2.	Drying (exclusive PVC)	Melting	Thermal model without consideration of kinetics
3.	Pyrolysis	Thermal decomposition	One-step model with Arrhenius approach
4.	Char conversion	-	kinetically/diffusively limited approach according to Baum and Street [3] and Field [4]

1.2 Heating

During heating, a heat balance is formed around the particle in order to calculate the internal temperature distribution, which serves as the starting point for the further conversion steps. To determine the temperature distribution, the particle is first discretized, followed by the solution of the one-dimensional heat conduction equation for a flat plate (see Eq. (1)) using the Crank-Nicolson method.

$$\frac{\partial T}{\partial t} = a_P \cdot \frac{\partial^2 T}{\partial x^2} \tag{1}$$

The Crank-Nicolson method is an established procedure for solving the one-dimensional heat conduction equation. Like other methods for discretizing differential equations (e.g., Euler explicit, Euler implicit), the method is based on a Taylor series expansion. Due to the temporal averaging of values at time n and n+1 (see Eq. (2)), the Crank-Nicolson method exhibits a second-order truncation error in time according to the Taylor series expansion. The higher the order of the truncation error, the more accurate the method. In addition to temporal averaging, a central difference is applied in space (see Eq. (3)), which also leads to a second-order truncation error with respect to space. The combination of Eq. (2) and Eq. (3) results in Eq. (4), which, due to its implicit nature, must be solved by a linear system of equations; the procedure used for this is discussed at the end of this section.

$$\frac{\partial T}{\partial t} = \frac{T^{n+1} - T^n}{\Delta t} = \frac{1}{2} \cdot \left[a_p \left(\frac{\partial^2 T^{n+1}}{\partial x^2} + \frac{\partial^2 T^n}{\partial x^2} \right) \right] \tag{2}$$

$$\frac{\partial^2 T}{\partial x^2} = \frac{T_{i+1} - 2T_i + T_{i-1}}{\Delta x^2} \tag{3}$$

$$\frac{T_i^{n+1} - T_i^n}{\Delta t} = \frac{1}{2} \cdot \left[a_p \left(\frac{T_{i+1}^{n+1} - 2T_i^{n+1} + T_{i-1}^{n+1}}{\Delta x^2} + \frac{T_{i+1}^n - 2T_i^n + T_{i-1}^n}{\Delta x^2} \right) \right] \tag{4}$$

Since the local derivative is a second-order differential equation, two boundary conditions are required to solve the one-dimensional heat conduction equation. The points at which the boundary conditions are implemented are marked accordingly in Figure 1 (b). Point 4 is needed to calculate the heat flux, which results from the temperature difference between the ambient temperature and the particle surface temperature. Based on Fourier's law, T_4 can be determined by forming a central difference in position (see Crank-Nicolson method). Building on this, equation Eq. (5) provides a general solution for implementing the heat flux density as a boundary condition, whereby *i* must be set to the outermost node of the particle at *h/2*. Assuming thermal symmetry around point 0 (i.e., $T_1 = T_{-1}$, etc.), the general form of the equation can be derived according to Eq. (6).

$$T_{\frac{h}{2}+1} = \frac{2 \cdot \Delta x \cdot \dot{q}}{\lambda_p} + T_{\frac{h}{2}-1} \tag{5}$$

$$T_i = T_{-i} \tag{6}$$

The heat conduction equation is first order with respect to time, which is why only one initial condition is required. During initialization, the temperatures at the nodes are set to an initial value (e.g., room temperature) once at the start of the simulation. The heat flow (convection + radiation + endothermic or exothermic processes) is then calculated based on the initial temperature of the particle. Heat transfer by convection occurs via the main surfaces of a plate and is determined according to equation Eq. (7), in which $A_{P,Main}$ is calculated using the term $2 \cdot l \cdot w$ and $T_{P,Surf}$ corresponds to the temperature at the particle surface in node $h/2$. To calculate the heat transfer coefficient (see Eq. (8), Nusselt correlations for a flat plate with longitudinal flow are used (see Eq. (9) - (Eq. (10)), whereby the plate length in the direction of flow l is used for the characteristic length L. Like the Reynolds number, the Nusselt number is a dimensionless parameter and describes how effectively heat is transferred by convection compared to conduction. In the transition range $10 < Re_P < 107$ (i.e., no purely turbulent flow has yet developed), the Nusselt number for a flat plate with longitudinal flow is determined by averaging according to equation Eq. (9). The Prandtl number, which describes the ratio between the velocity boundary layer surrounding the particle and the temperature boundary layer, is calculated as the quotient of the kinematic viscosity v_g and the thermal diffusivity a_g (see (Eq. 39)) [118].

$$\dot{Q}_{Conv} = \alpha \cdot A_{P,Main} \cdot (T_g - T_{P,Surf}) \tag{7}$$

$$\alpha = \frac{Nu \cdot \lambda_g}{L} = \frac{Nu \cdot \lambda_g}{l} \tag{8}$$

$$Nu = \sqrt{{Nu_{lam}}^2 + {Nu_{turb}}^2} \tag{9}$$

$$Nu_{lam} = 0{,}644 \cdot {Re_P}^{1/2} \cdot Pr^{1/3} \tag{10}$$

$$Nu_{turb} = \frac{0{,}037 \cdot {Re_P}^{0,8} \cdot Pr}{1+2{,}443 \cdot {Re_P}^{-0,1}(Pr^{2/3}-1)} \tag{11}$$

$$Pr = \frac{\nu_g}{a_g} \tag{12}$$

The transmitted radiant heat flux is calculated based on the effective radiation temperature T_{eff} according to equation Eq. (13). The effective radiation temperature is a theoretical quantity that corresponds to the temperature of an ideal black body that emits exactly the radiation power that the object under consideration (e.g., an RDF particle) receives from its environment. It is derived from the irradiance G incident on the particle and the geometry of the particle. In G, the heat flux densities supplied by radiation from all incident rays from all spatial directions are combined into a scalar value. The flat RDF particle transfers heat analogously to the convection already considered, only via the two main surfaces $2 \cdot l \cdot w$. In contrast to convection, where a directed flow/heat transfer has been assumed, the thermal radiation hits the particle in a non-directional manner from all spatial directions. The complex and computationally intensive conversion of G into directed rays that strike only the main surfaces has been omitted here. Instead, the RDF particle is considered a sphere with a uniform surface for the purpose of calculating the amount of heat transferred

within this modeling step. Due to the thermal symmetry of the particle mentioned above, a homogeneous radiation field is assumed, in which the incoming radiant heat heats the particle evenly. The incoming rays act on the projected area $\pi \cdot r_{eq}^2$ orthogonally to the direction of incidence. Added together, this results in the heat flux $G \cdot \pi \cdot r_{eq}^2 \cdot \alpha_p$ absorbed by the particle. The emitted heat is distributed evenly over the surface of the particle according to the expression $\sigma \cdot 4 \cdot \pi \cdot r_{eq}^2 \cdot \varepsilon_p \cdot T_{Eff}$. For each time step, a radiation equilibrium between the thermal radiation absorbed by the particle and that emitted by it is assumed. Due to the radiation equilibrium, according to Kirchhoff, $\alpha_p = \varepsilon_p$, which results in equation Eq.(13). In the radiation equilibrium, it is assumed that the temperature of the particle surface corresponds to T_{eff}, which is not the case in reality. This results in a difference between T_{eff} and $T_{P,Surf,}$ whereby the amount of equation Eq. (14) can be interpreted as a deviation from the radiation equilibrium between the particle and its environment. This approach takes into account the transient, radiation-induced heating of the particle.

$$T_{Eff} = \left(\frac{G}{4 \cdot \sigma}\right)^{1/4} \tag{13}$$

$$\dot{Q}_{Rad} = \sigma \cdot \varepsilon_P \cdot A_{P,Main} \cdot \left(T_{Eff}{}^4 - T_{P,Surf}{}^4\right) \tag{14}$$

The heat flows from endothermic or exothermic processes (such as drying, pyrolysis, residual char combustion, melting, thermal decomposition, or homogeneous gas phase reaction) that heat up or cool down the particles depend on the mass conversion and enthalpy of the respective reaction step and are calculated using equations Eq. (15) - Eq.(20).

$$\dot{Q}_{Drying} = \frac{m_{Steam} \cdot \Delta h_{Drying}}{\Delta t} \tag{15}$$

$$\dot{Q}_{Pyr} = \frac{m_{vol,released} \cdot \Delta h_{Pyr}}{\Delta t} \tag{16}$$

$$\dot{Q}_{Ox} = \frac{m_C \cdot \Delta h_{Ox}}{\Delta t} \tag{17}$$

$$\dot{Q}_{Melting} = \frac{m_{Melting} \cdot \Delta h_{Melting}}{\Delta t} \tag{18}$$

$$\dot{Q}_{Decomp} = \frac{m_{Decomp} \cdot \Delta h_{Decomp}}{\Delta t} \tag{19}$$

$$\dot{Q}_{Gasphase} = \frac{m_{C_2H_4} \cdot \Delta h_{C_2H_4} + m_{CH_4} \cdot \Delta h_{CH_4} + m_{C_2H_2} \cdot \Delta h_{C_2H_2}}{\Delta t} \tag{20}$$

The total heat flux transferred to the particle is the sum of the individual heat fluxes (from convection, radiation, drying, etc.) and is used to calculate the new particle temperatures

T_i that will be present in the next time step. According to Eq. (5), this requires knowledge of the heat flux density, which can be calculated using equation Eq. (21).

$$\dot{q} = \frac{\dot{Q}_{total}}{A_{P,Main}} \tag{21}$$

The determined heat flux density provides all the information needed to set up the linear equation system by inserting the respective nodes for *i* into Eq. (4) and entering the corresponding boundary conditions. Since the initial condition is only required for the initial simulation step, the newly calculated temperatures T_i provide the initial values for the subsequent time step. The resulting linear equation system is a tridiagonal matrix that is solved using the Thomas algorithm. This algorithm is particularly suitable for tridiagonal matrices, as fewer arithmetic operations are required compared to classical Gaussian elimination.

1.3 Drying

The mass of water passing from the particle into the vapor phase per time step is calculated using a drying front that moves through the particle. This assumes that the initial mass of water is evenly distributed across the individual shells of the particle. In contrast to the volatile compounds released during pyrolysis, the water present in the particle is only weakly bound. Therefore, kinetic parameters are not taken into account when modeling the drying process. Instead, a purely thermal model is used, which assumes instantaneous evaporation of the water when the drying temperature is reached. The drying progress depends exclusively on the local temperature distribution and the number of nodes defined by discretization. The expansion of the drying front h^*_{Drying} is determined by linear interpolation between the temperatures T_i and the node ratios ψ_i of successive nodes (see Eq. (22). The node ratio compares the number of the node currently being considered with the total number of nodes and serves as a dimensionless measure for dividing the particle into sections. The drying temperature T_{drying} describes the particle temperature at which the endothermic drying process begins and is defined as 100 °C. The values for h^*_{Drying} vary between 1 and 0, where 1 corresponds to a completely undried state and 0 to a completely dried state.

$$h^*_{Drying} = \frac{\psi_{i+1} - \psi_i}{T_{i+1} - T_i} \cdot T_{Drying} + \left(\psi_i - \frac{\psi_{i+1} - \psi_i}{T_{i+1} - T_i} \cdot T_i\right) \tag{22}$$

With the help of the drying front, the dried mass of water for the current time step *n* can then be calculated see Eq. (23). For better differentiation, the water that has transitioned into the gas phase is referred to as steam, and the water that remains in the particle is referred to as water. At the initial start of the simulation, no water has yet evaporated, so the value of m_{Steam}^{n-1} is zero.

$$m_{Steam}^{\ n} = m_{Water,ini} \cdot \left(1 - h^*_{Drying}\right) - m_{Steam}^{\ n-1} \tag{23}$$

Only the maximum amount of water valid for each shell can be evaporated per shell. The total amount of water evaporated is continuously accumulated and cannot exceed the initial amount of water bound. At the same time, the total mass of the particle is reduced by the amount of water evaporated per time step. During the drying process, the particle volume is assumed to remain constant, which is why the density of the particle must also be adjusted after each time step.

1.4 Pyrolysis

In pyrolysis, when the material-specific pyrolysis temperature T_{Pyr} is reached, the immediate release of volatiles is not assumed, as is the case with drying, but the kinetics of the process are taken into account. For better differentiation, the components that have already transitioned into the gas phase are referred to here as volatiles, and the components still bound in the particle are referred to as volatiles. The initial mass of the volatiles is distributed evenly across the individual shells, just like the mass of water present in the particle. In order to reduce the complexity of the pyrolysis process, a one-step model has been chosen in which no distinction is made between primary and secondary pyrolysis. In the model, the mass of volatiles released per time step by pyrolysis is calculated using an Arrhenius approach. First, the rate constant $k_{vol,i}$ of the corresponding shell is calculated as a function of T_i in equation Eq. (24), whereby the kinetic parameters k_0 and E_A used must be selected specifically for the material. The mass of volatiles released per shell is then calculated see Eq. (25). The mass of volatiles present per shell is adjusted as the simulation progresses in accordance with equation Eq. (26). The cumulative mass of volatiles is calculated by continuously adding up the masses volatilized per time step. The latter are determined by the sum of the volatiles degassed per shell and time step. The volume fraction φ_i of a single shell in the total volume (which has already been implicitly taken into account in the description of the uniform distribution of water and volatiles in the particle) is determined using the known node ratios and the external dimensions of the particle.

$$k_{vol,i} = k_{0,vol} \cdot e^{-\frac{E_{A,vol}}{R \cdot T_i}} \tag{24}$$

$$m_{vol,released,i} = m_{vol,bounded,i} \cdot k_{vol,i} \cdot \Delta t \tag{25}$$

$$m_{vol,bounded,i} = \varphi_i \cdot m_{vol,bounded,ini} - m_{vol,released,cumulated,i} \tag{26}$$

Similar to drying, only a maximum permissible mass of volatiles can be degassed per shell. The total release of volatiles beyond the value of the initial mass of volatiles is not possible.

Equivalent to the drying process, a constant volume is assumed during pyrolysis. In addition to the decreasing total mass, this also means that the density of the particle must be recalculated after each time step.

During the pyrolysis of biogenic fractions, no change in shape is assumed and the particle remains in the plate shape shown in Figure 1(b). During the thermal conversion of PVC, however, a change in the shape of the particle is assumed once 50% of the volatile mass has been released: the resulting residual char contracts due to ongoing aromatization processes, meaning that the particle is considered to be spherical from this point onwards. The change in shape means that the one-dimensional heat conduction equation must be adapted for a spherical geometry. Instead of the main surfaces of the flat plate, the surface of the sphere with the same volume is now considered the heat transfer surface, which also means that the routines for heat transfer by convection and radiation must be adapted. In addition, the characteristic length must be chosen as the diameter of the sphere of equal volume, and the Nusselt and Sherwood correlations must be modified. In order to maintain the readability of this handout while ensuring the completeness of the equations, the aforementioned correlations are listed in the appendix.

In contrast to Liedmann [1], this study rejects the pseudo-species approach based on the $C_xH_yO_z$ scheme and advocates the use of clearly defined pyrolysis gases (CO_2, CO, CH_4, H_2, H_2O for biogenic materials [5] and HCl, CO_2, CH_4, C_2H_2 for PVC [6]) for calculating the homogeneous gas phase reaction: The use of fixed species makes it possible to use polynomials to describe the temperature dependence of material properties (e.g., heat capacities and formation enthalpies); no such database exists for “artificially” composed pseudo-species. In addition, parameters relating to kinetics are available for fixed species for calculating conversion rates, which are unknown for composite pseudo-species. Although pseudo-species of the form $C_xH_yO_z$ are suitable for fulfilling the mass/element and energy balance, this can also be achieved by a suitable composition of the pyrolysis gases. From a global perspective, pyrolysis is an endothermic process, but exothermic partial reactions are also possible within it.

1.5 Residual-Char Combustion

When the oxidation temperature T_{Ox} is reached, exothermic residual char combustion only takes place on the surface of the particle, meaning that the intra-particle temperature distribution plays no role in this case. The model used, based on Baum and Street [3] and Field [4], was developed specifically for the combustion of spherical coal particles, which is why equation Eq. (27) has been supplemented by a material-specific factor χ that takes into account the deviation from the ideal coal particle. The parameters K and ζ associated with χ see (28) are determined on the basis of post-simulation analyses of the burn-off behaviour of model fuels and are then used to model the conversion characteristics of real RDF particles. Since the model is a kinetically/diffusively limited approach, the influence of the respective proportions c_{Diff} (see Eq. (29)) and c_{Chem} (see Eq. (30)) is weighted by the

formation of the harmonic mean. The proportion c_{Diff} representing diffusion is calculated using the mass transfer coefficient β and the proportion relating to the chemical reaction is calculated using an Arrhenius approach. This work assumes that the RDF particles are completely oxidized to C_{O2}. Both the pyrolysis and oxidation of carbon to C_{O2} are considered first-order reactions, but there are differences in the description of the pre-exponential factor in the Arrhenius equation: Since the carbon contained in the residual char is present together with ash residues, the fixed amount of carbon cannot be directly recorded as a molar number. Accordingly, the reaction kinetics are formulated in terms of mass. In contrast to pyrolysis, which takes place over the entire particle volume, residual char combustion occurs exclusively on the particle surface. For this reason, the pre-exponential factor is related to the surface of the particle. In addition, the reaction process depends on the partial pressure of oxygen, which is therefore explicitly included in the mathematical description. To calculate the mass transfer coefficient β (see Eq. (31)), the Sherwood number *Sh* (see Eq. (32)) is required, which is determined depending on the geometry using the correlation for a flat plate or sphere. The Schmidt number according to equation Eq. (33) is used to calculate the Sherwood number. Both quantities are dimensionless parameters, with the Sherwood number and Schmidt number representing the mass transfer counterparts to the Nusselt and Prandtl numbers. The diffusion coefficient required for the calculation (see Eq. (34)) depends on pressure and temperature and is determined on the basis of reference values. The model approach used assumes that the particle retains its cuboid geometry (in the case of biogenic materials) or its spherical geometry (in the case of PVC) and that the density of the particle remains constant. This information can be used to recalculate the particle volume after each time step. Assuming that biogenic particles retain their initial side length ratios during residual char combustion, the current side lengths and surface area can be calculated using the known volume.

$$m_{Ox} = \frac{A_P}{\frac{1}{c_{Diff}} + \frac{1}{c_{Chem}}} \cdot p_{O_2,g} \cdot \chi \cdot \Delta t \tag{27}$$

$$\chi = \frac{1}{K \cdot {x_{O_2,g}}^{\zeta}} \tag{28}$$

$$c_{Diff} = \frac{M_C \cdot \beta}{R \cdot T_m} \tag{29}$$

$$c_{Chem} = k_c \cdot e^{-\frac{E_{A,Ox}}{R \cdot T_{Surf}}} \tag{30}$$

$$\beta = \frac{Sh \cdot D_{O_2}}{L} = \frac{Sh \cdot D_{O_2}}{l} \tag{31}$$

$$Sh = 0{,}644 \cdot {Re_P}^{1/2} \cdot {Sc}^{1/3} \tag{32}$$

$$Sc = \frac{\nu_g}{D_{O_2}} \tag{33}$$

$$D_{O_2} = D_{O_2,ref} \cdot \left(\frac{p_{g,ref}}{p_g}\right) \cdot \left(\frac{T_g}{T_g,ref}\right)^{1,75} \quad (34)$$

1.6 Melting

Only thermoplastics and thermoplastic elastomers are capable of melting, as the individual polymers are only loosely connected to each other via van der Waals forces or isolated covalent bonds. This is also the reason why this modeling approach, as in the case of drying, assumes a thermal model with immediate execution of the conversion step when the corresponding temperature is reached. The procedure for calculating the dimensionless melt front is similar to the procedure for calculating the drying front, taking into account the melting temperature T_{Melt}(see Eq. (35)).

$$h^*_{Melting} = \frac{\psi_{i+1} - \psi_i}{T_{i+1} - T_i} \cdot T_{Melting} + (\psi_i - \frac{\psi_{i+1} - \psi_i}{T_{i+1} - T_i} \cdot T_i) \quad (35)$$

During melting, no species are transported into the gas phase. In addition to the endothermic phase transformation, the central importance of the melting process for thermal conversion lies in the change in particle geometry: According to Liedmann [1], the shape transformation begins as soon as 50 % of the particle has melted. The unmelted portion of the RDF particle changes from an aspherical to a more spherical shape. In the case of Liedmann [1], however, the particle never reaches a spherical shape, but remains a cuboid due to the adjustment of the side length ratios. This paper does not use the approximation formulas established by Liedmann [1] to calculate the side length ratios. Instead, the particle is considered an ideal sphere as soon as the melt front reaches or falls below 50 %. The transformation from solid plastic to melt is based on the shrinking core model: The melting process is considered to progress from the outside in, with the volume of the respective particle geometry remaining constant and the solid core shrinking as the melt increases (see Figure 2).

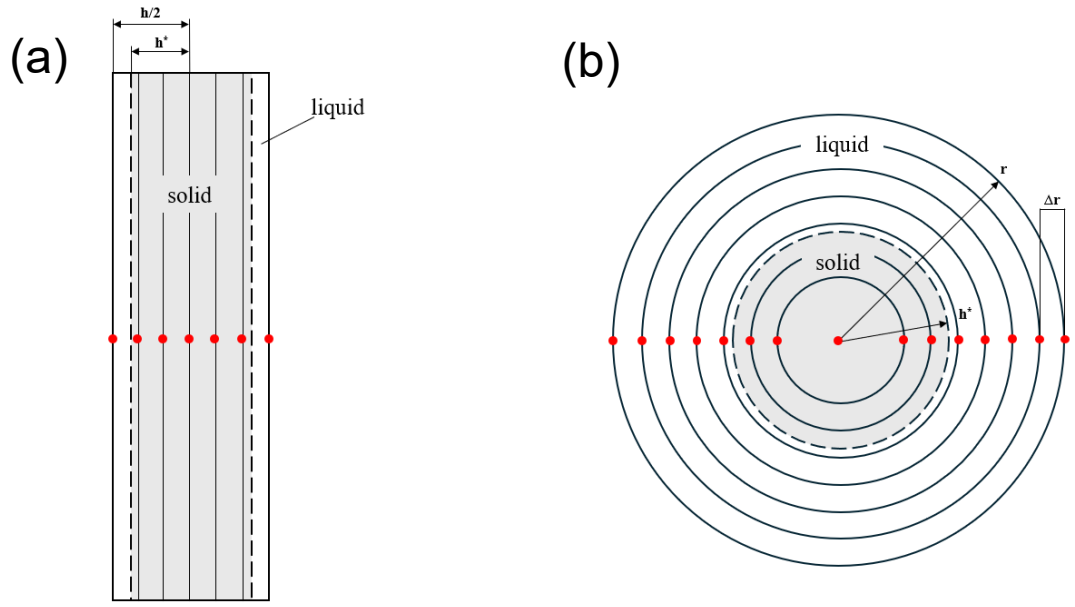

Figure 2: Change in shape due to melting: (a) Original view as a plate; (b) as soon as the melt front reaches or falls below 50 %, the particle is geometrically regarded as a sphere [2].

With regard to the change in shape, equation Eq. (36)) for calculating the molten particle mass must be adjusted: After the change in shape has occurred, the melt front no longer contributes to the melting of the particle in a one-dimensional manner, but rather in a three-dimensional manner in accordance with the relationship for calculating the sphere volume (see Eq. (37)).

$$m_{Melted}{}^{n} = m_{P,ini} \cdot \left(1 - h^{*}{}_{Melting}\right) - m_{Melted}{}^{n-1}; \qquad 1 > m_{Melted} > 0.5 \qquad (36)$$

$$m_{Melted}{}^{n} = m_{P,ini} \cdot \left(1 - h^{*}{}_{Melting}{}^{3}\right) - m_{Melted}{}^{n-1}; \qquad 0{,}5 \geq m_{Melted} \geq 0 \qquad (37)$$

Further adjustments due to the change in shape of the PE must be made in the routine for heating the particle in the same way as for the change in shape of PVC (see section on pyrolysis in this chapter).

1.7 Thermal Decomposition

The thermal decomposition of PE is modeled equivalently to pyrolysis using a one-step model including the Arrhenius approach, which leads to equation Eq. (38). It is assumed that the liquid melt continues to envelop the particle and thus the shell model concept still applies (see Figure 2(b)). It should be noted here that the material values change as a result of the phase transition and thus influence the heat transport in the particle. Once T_i

has reached or exceeded the decomposition temperature, volatiles are transferred endothermically from the melt to the gas phase based on the approach of Liedmann [1]. According to Matthiesen et al. [225], primarily C_2H_4, CH_4, and C_2H_2 are released, which is why the modeling is limited to these species. During the decomposition process, the mass of liquid PE decreases, but not the mass of solid PE, which is why the newly adjusted particle volume is calculated using the masses and densities of the subphases. The decomposition process continues until the entire melt is used up (see Eq. (39)).

$$k_{Decomp,i} = k_{0,Decomp} \cdot e^{-\frac{E_{A,Decomp}}{R \cdot T_i}} \tag{38}$$

$$m_{Decomp,i} = m_{Decomp,i} \cdot k_{Decomp,i} \cdot \Delta t \tag{39}$$

1.8 Gasphase reaction

The homogeneous gas phase reaction for converting the species released by pyrolysis (biogenic materials and PVC) takes place via the eddy dissipation concept (EDC) according to Magnussen. The speed of thermal conversion depends on the type of flow (turbulent flows ensure better mixing of oxidizer and fuel) and the kinetics of the chemical reaction. The EDC takes both aspects into account: using a turbulence model, the simulation domain is divided into areas of coarse and finer vortex structures. The chemical processes for converting the species take place in the finer structures, which are on the scale of molecules. In contrast to the eddy dissipation model (EDM), which assumes an infinitely fast reaction rate and works according to the principle of “mixed equals burned”, EDC takes into account the actual reaction kinetics and thus the temporal conversion of the individual species. The heat energy released during the chemical conversion is implicitly taken into account via the new temperature of the CFD cell in which the particle is located.

A hybrid approach combining EDC and boundary layer reaction is chosen to model the homogeneous conversion of species originating from thermal decomposition (PE). Boundary layer reaction is understood here to mean that the species react in the immediate vicinity of the particle, provided that the diffusive oxygen transport to the particle surface is large enough. In this case, the species are not introduced into the CFD domain (and converted there via EDC), but are converted directly at the particle surface. Since the use of EDC averages the heat released by the homogeneous reaction over the entire CFD cell in which the particle is located, the heat output actually transferred to the particle surface is insufficiently recorded: In the case of PE particles, the flame is located at the particle surface compared to biogenic particles and PVC; However, when EDC is used alone, the flame is extended to the entire CFD cell. Accordingly, it is not possible to reproduce reactions occurring in the boundary layer via EDC. In order to still map reactions in the immediate surface area of the particle and establish a mathematical relationship to the oxygen partial pressure (for biogenic particles and PVC, this is done using the routine for residual

char combustion), the EDC is expanded in accordance with the following concept. The concept is based on Fick's first law $\frac{dn_{O_2}}{dt} = -D_{O_2} \cdot A_p \cdot \frac{\partial c_{O_2}}{\partial x}$, which is used to calculate the diffusive oxygen transport from the atmosphere surrounding the particle (outside the particle's sphere of influence) to the particle surface. The differential ∂c_{O_2} is expressed in terms of the oxygen concentration surrounding the particle and the oxygen concentration at the particle surface, which is approximated to zero. Consequently, ∂x is described by the boundary layer thickness δ, which can be calculated using the definition of the mass transfer coefficient $\beta_{O_2} = \frac{D_{O_2}}{\delta}$. Using the ideal gas law and Dalton's law, the concentration c_{O_2} is reformulated to the partial pressure p_{O_2}. By finally multiplying Fick's law by the molar mass of oxygen M_{O_2} and the time interval Δt under consideration, the mass of oxygen diffusing into the boundary layer is determined (see Eq. (40)).

$$m_{GS,O_2} = \beta_{O_2} \cdot A_P \cdot M_{O_2} \cdot \frac{p_{O_2}}{R \cdot T} \cdot \Delta t \tag{40}$$

Depending on whether the particle still exists as a plate or has already melted into a sphere, the corresponding correlation of the Sherwood number is used to calculate the mass transfer coefficient. Based on the respective reaction equations, the converted species masses are determined, and the reaction enthalpy released in the process is explicitly used to heat the particle. The order of the degassing process is important here, as the respective mass of reacted species depends on the oxygen diffusing into the boundary layer. First, C_2H_4 is released, followed by CH_4 and C_2H_2 [7]. If there is no more oxygen available to oxidize the degassing species directly in the boundary layer, they are transferred to the CFD domain and converted via the EDC. In formulating equation Eq. (40), a conscious decision was made against the molar-based variant, as the DEM simulation framework works with mass source terms rather than molar source terms.

2 References

[1] Birk Liedmann, *Simulation der thermischen Umsetzung flugfähiger Ersatzbrennstoffe in Drehrohröfen der Zementindustrie*, Shaker Verlag, Aachen, 2018.

[2] Streier, R., *Untersuchung des Flug- und Abbrandverhaltens von Ersatzbrennstoffen (EBS) zur thermischen Nutzung in Zement-Drehrohröfen unter stark überstöchiometrischen Oxyfuel-Bedingungen (in Bearbeitung)*, Bochum, Dezember 2025.

[3] BAUM, M. M., and STREET, P. J., "Predicting the Combustion Behaviour of Coal Particles," *Combustion Science and Technology*; Vol. 3, No. 5, 1971, pp. 231–243. doi: 10.1080/00102207108952290.

[4] Field, M. A., "Rate of combustion of size-graded fractions of char from a low-rank coal between 1 200°K and 2 000°K," *Combustion and Flame*; Vol. 13, No. 3, 1969, pp. 237–252. doi: 10.1016/0010-2180(69)90002-9.

[5] Mehrabian, R., Shiehnejadhesar, A., Scharler, R., and Obernberger, I., "Multi-physics modelling of packed bed biomass combustion," *Fuel*; Vol. 122, 2014, pp. 164–178. doi: 10.1016/j.fuel.2014.01.027.

[6] Li, W., Bai, Z., Zhang, T., Jia, Y., Hou, Y., Chen, J., Guo, Z., Kong, L., Bai, J., and Li, W., "Comparative study on pyrolysis behaviors and chlorine release of pure PVC polymer and commercial PVC plastics," *Fuel*; Vol. 340, 2023, p. 127555. doi: 10.1016/j.fuel.2023.127555.

[7] Matthiesen, K., Plessing, L., and Luinstra, G. A., "Fast Pyrolysis Product Analysis of Commercial Polyethylenes," *Energy & Fuels*; Vol. 38, No. 16, 2024, pp. 15543–15559. doi: 10.1021/acs.energyfuels.4c02296.

Appendix

Heat conduction equation including discretization using the Crank-Nicolson method for a sphere

$$\frac{\partial T}{\partial t} = a_P \cdot \frac{\partial^2 T}{\partial r^2} + \frac{2a_P}{r} \cdot \frac{\partial T}{\partial r}$$

$$\frac{\partial T}{\partial t} = \frac{T^{n+1} - T^n}{\Delta t} = \frac{1}{2} \cdot \left[a_P \left(\frac{\partial T^{n+1}}{\partial r^2} \right) + \frac{2a_P}{r} \left(\frac{\partial T^{n+1}}{\partial r} \right) + a_P \left(\frac{\partial^2 T^n}{\partial r^2} \right) + \frac{2a_P}{r} \left(\frac{\partial T^n}{\partial r} \right) \right]$$

$$\frac{\partial T}{\partial r} = \frac{T_{i+1} - T_{i-1}}{2\Delta r}$$

$$\frac{\partial^2 T}{\partial r^2} = \frac{T_{i+1} - 2T_i + T_{i-1}}{(\Delta r)^2}$$

$$\frac{T^{n+1} - T^n}{\Delta t} = \frac{1}{2} \cdot \left[a_P \left(\frac{T_{i+1}^{n+1} - 2T_i^{n+1} + T_{i-1}^{n+1}}{(\Delta r)^2} \right) + \frac{2a_P}{r} \left(\frac{T_{i+1}^{n+1} - T_{i-1}^{n+1}}{2\Delta r} \right) + a_P \left(\frac{T_{i+1}^{n} - 2T_i^{n} + T_{i-1}^{n}}{(\Delta r)^2} \right) + \frac{2a_P}{r} \left(\frac{T_{i+1}^{n} - T_{i-1}^{n}}{2\Delta r} \right) \right]$$

First boundary condition: Thermal symmetry (i.e., $T_1 = T_{-1}$ etc.) around the center of the sphere, simplifying the heat conduction equation to determine T_0 by considering the limit according to L'Hospital's rule.

$$\frac{\partial T}{\partial t} = \lim_{n \to 0} \frac{g(r)}{h(r)} = \lim_{n \to 0} \frac{g'(r)}{h'(r)} = \frac{a_P \cdot \frac{\partial^2 T}{\partial r^2} \cdot r + 2a_P \cdot \frac{\partial T}{\partial r}}{r} = 3a_P \cdot \frac{\partial^2 T}{\partial r^2}$$

Second boundary condition: Incorporation of the heat flux density using Fourier's law at $i = r$

$$T_{r+1} = \frac{2 \cdot \Delta r \cdot \dot{q}}{\lambda_p} + T_{r-1}$$

Heat transfer by convection and radiation for a sphere

$\dot{Q}_{Conv} = \alpha \cdot A_P \cdot (T_g - T_{P,Surf})$
$\dot{Q}_{Str} = \sigma \cdot \varepsilon_P \cdot A_P \cdot ({T_{Eff}}^4 - {T_{P,Surf}}^4)$
Mit $A_P = \pi \cdot {d_{eq}}^2$
Nusselt correlation for calculating the heat transfer coefficient for a sphere
$\alpha = \frac{Nu \cdot \lambda_g}{L} = \frac{Nu \cdot \lambda_g}{d_{eq}}$
$Nu = 2 + \sqrt{{Nu_{lam}}^2 + {Nu_{turb}}^2}$
Nu_{lam} and Nu_{turb} continue to be calculated according to the mentioned equations, whereby the Reynolds number is now calculated using the equivalent diameter of the sphere with the same volume.
Sherwood correlation for calculating the mass transfer coefficient for a sphere
$\beta = \frac{Sh \cdot L}{D} = \frac{Sh \cdot d_{eq}}{D}$
$Sh = 2 + 0{,}6 \cdot Re^{1/2} \cdot Sc^{1/3}$
The Reynolds number is now calculated using the equivalent diameter of the sphere with the same volume.